



ELSEVIER

Comput. Methods Appl. Mech. Engrg. 156 (1998) 259–276

**Computer methods
in applied
mechanics and
engineering**

A consistent finite element formulation for linear buckling analysis of spatial beams

K.M. Hsiao*, R.T. Yang, W.Y. Lin

Department of Mechanical Engineering, National Chiao Tung University, Hsinchu, Taiwan, ROC

Received 17 March 1997; revised 15 May 1997

Abstract

A consistent co-rotational finite element formulation and numerical procedure for the linear buckling analysis of three-dimensional elastic Euler beam is presented. A mechanism for generating configuration dependent conservative moment is proposed and the corresponding load stiffness matrix is derived. It is assumed that the prebuckling displacements and rotations of the structure and the corresponding deformations of the elements are linearly proportional to the external loading. The prebuckling rotations of the structure are fixed axis rotations or small rotations, and the effect of the prebuckling displacement on transformation matrix for the coordinates transformation can be ignored. All coupling among bending, twisting and stretching deformations for beam element is considered by consistent linearization of the fully geometrically nonlinear beam theory. An inverse power method for the solution of the generalized eigenvalue problem is used to find the buckling load and buckling mode. Numerical examples are presented to demonstrate the accuracy and efficiency of the proposed method. © 1998 Elsevier Science S.A.

1. Introduction

The linear buckling analysis has been the subject of considerable research, and many valuable results have been reported in the literature [1–13]. The buckling of the beam structures is caused by the coupling among bending, twisting and stretching deformations of the beam members. Thus, the buckling analysis is known as a second-order analysis [1]. In order to capture correctly all coupling among bending, twisting and stretching deformations of the beam elements, the formulation of beam elements might be derived by consistent linearization of the fully geometrically nonlinear beam theory [14]. However, the governing equations of conventional linear buckling analysis are not derived from the consistent linearization of the fully geometrically nonlinear beam theory. Thus, the conventional linear buckling analysis cannot account for the complete deformational coupling. A large number of nonlinear models of thin-walled beams has been proposed (e.g. see the references in [15]). However, most of them are applied to the non-linear analysis of beams. Their application in the linear buckling analysis has been rather limited (e.g. [12,13]). To the authors' knowledge, it seems that their governing equations are not obtained by consistent linearization of the fully geometrically nonlinear beam theory. The objective of this study is to present a consistent co-rotational finite element formulation and numerical procedure for the linear buckling analysis of three-dimensional elastic Euler beam using consistent linearization of the fully geometrically nonlinear beam theory. In [16], Hsiao presented a co-rotational total Lagrangian formulation of beam element for the nonlinear analysis of three-dimensional beam structures with large rotations but small strains. All coupling among bending, twisting and stretching deformations for beam element is correctly considered by the fully geometrically nonlinear beam theory. Element deformations and

* Corresponding author.

element equations are defined in terms of element coordinates which are constructed at the current configuration of the beam element. The element deformations are determined by the rotation of element cross section coordinates, which are rigidly tied to element cross section, relative to the element coordinate system. In conjunction with the co-rotational formulation, the higher-order terms of nodal parameters in element nodal force and stiffness matrix are consistently dropped. It seems that this element can be adapted for the linear buckling analysis of the beam structures. Thus, the beam element presented in [16] is modified and employed here.

The configuration dependent conservative moment is considered and the corresponding load stiffness matrix is derived. It is assumed that the prebuckling displacements and rotations of the structure and the corresponding deformations of the elements are linearly proportional to the external loading. The prebuckling rotations of the structure are fixed axis rotations or small rotations, and the effect of the prebuckling displacement on transformation matrix for the coordinates transformation can be ignored. An inverse power method for the solution of the generalized eigenvalue problem is used to find the buckling load and buckling mode. Numerical examples are presented to demonstrate the accuracy and efficiency of the proposed method.

2. Finite element formulation

In the following only a brief description of the beam element is given. The more detailed description may be obtained from [16].

2.1. Basic assumptions

The following assumptions are made in derivation of the beam element behavior.

- (1) The beam is prismatic and slender, and the Euler–Bernoulli hypothesis is valid.
- (2) The cross section of the beam is doubly symmetric.
- (3) The unit extension and the twist rate of the centroid axis of the beam element are uniform.
- (4) The cross section of the beam element does not deform in its own plane and strains within this cross section can be neglected.
- (5) The out-of-plane warping of the cross section is the product of the twist rate of the beam element and the Saint Venant warping function for a prismatic beam of the same cross section.
- (6) The deformations of the beam element are small.

2.2. Coordinate systems

In this paper, a co-rotational total Lagrangian formulation is adopted. In order to describe the system, we define four sets of right handed rectangular Cartesian coordinate systems:

- (1) A fixed global set of coordinates, X_i^G ($i = 1, 2, 3$) (see Fig. 1); the nodal coordinates, displacements, and rotations, and the stiffness matrix of the system are defined in this coordinates.
- (2) Element cross section coordinates, x_i^S ($i = 1, 2, 3$) (see Fig. 1); a set of element cross section coordinates is associated with each cross section of the beam element. The origin of this coordinate system is rigidly tied to the shear center of the cross section. The x_1^S axes are chosen to coincide with the normal of the unwrapped cross section and the x_2^S and x_3^S axes are chosen to be the principal directions of the cross section.
- (3) Element coordinates, x_i ($i = 1, 2, 3$) (see Fig. 1); a set of element coordinates is associated with each element, which is constructed at the current configuration of the beam element. The origin of this coordinate system is located at node 1, and the x_1 axis is chosen to pass through two end nodes of the element; the x_2 and x_3 axes are chosen to be the principal directions of the cross section at the undeformed state. *Note that this coordinate system is a local coordinate system not a moving coordinate system.* The deformations, internal nodal forces and stiffness matrix of the elements are defined in terms of these coordinates. In this paper the element deformations are determined by the rotation of element cross section coordinate systems relative to this coordinate system.

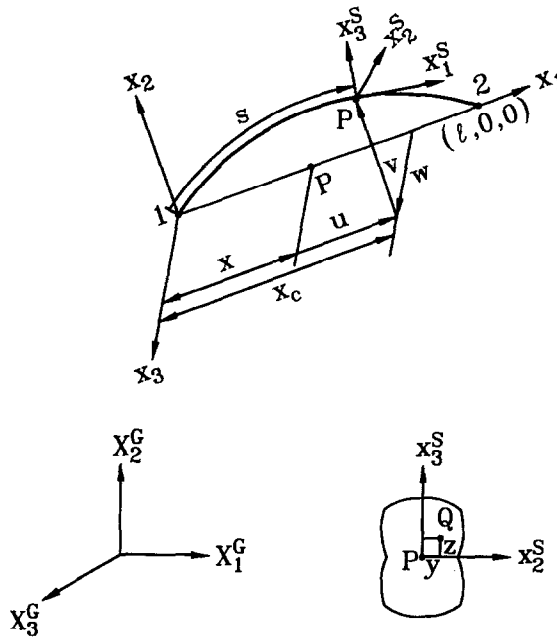


Fig. 1. Coordinate systems.

(4) Load base coordinates, X_i^P ($i = 1, 2, 3$); a set of load base coordinates is associated with each configuration dependent moment. The origin of this coordinate system is chosen to be the node where the configuration dependent moment is applied. The mechanism for generating configuration dependent moment is described in this coordinates, and the corresponding external load and load stiffness matrix are defined in terms of this coordinates.

In this paper, the symbol $\{ \}$ denotes column matrix. The relations among the global coordinates, element cross section coordinates, element coordinates and load base coordinates may be expressed by

$$X^G = A_{GS}x^S, \quad X^G = A_{GE}x, \quad X^G = A_{GP}X^P \tag{1}$$

where $X^G = \{X_1^G, X_2^G, X_3^G\}$, $x^S = \{x_1^S, x_2^S, x_3^S\}$, $x = \{x_1, x_2, x_3\}$, and $X^P = \{X_1^P, X_2^P, X_3^P\}$; A_{GS} , A_{GE} and A_{GP} are matrices of direction cosines of the element cross section coordinate system, element coordinate system, and load base coordinate system, respectively.

2.3. Rotation vector and rotation parameters

For convenience of the later discussion, the term ‘rotation vector’ is used to represent a finite rotation. Fig. 2 shows that a vector \mathbf{b} which as a result of the application of a rotation vector $\phi\mathbf{a}$ is transported to the new position $\bar{\mathbf{b}}$. The relation between $\bar{\mathbf{b}}$ and \mathbf{b} may be expressed as [17]

$$\bar{\mathbf{b}} = \cos \phi \mathbf{b} + (1 - \cos \phi)(\mathbf{a} \cdot \mathbf{b})\mathbf{a} + \sin \phi(\mathbf{a} \times \mathbf{b}) \tag{2}$$

where ϕ is the angle of counterclockwise rotation, and \mathbf{a} is the unit vector along the axis of rotation.

Let \mathbf{e}_i and \mathbf{e}_i^S ($i = 1, 2, 3$) denote the unit vectors associated with the x_i and x_i^S axes, respectively. Here, the triad \mathbf{e}_i^S in the deformed state is assumed to be achieved by the successive application of the following two rotation vectors to the triad \mathbf{e}_i :

$$\theta_n = \theta_n \mathbf{n} \tag{3}$$

and

$$\theta_t = \theta_t \mathbf{t} \tag{4}$$

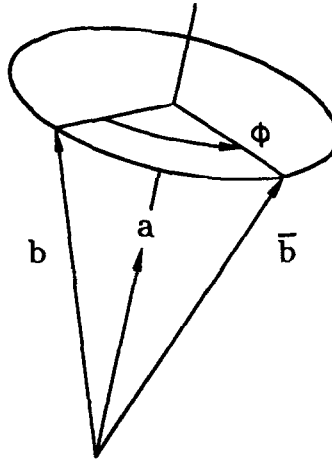


Fig. 2. Rotation vector.

where

$$\begin{aligned}
 \mathbf{n} &= \{0, \theta_2 / (\theta_2^2 + \theta_3^2)^{1/2}, \theta_3 / (\theta_2^2 + \theta_3^2)^{1/2}\} \\
 &= \{0, n_2, n_3\}
 \end{aligned}
 \tag{5}$$

$$\mathbf{t} = \{\cos \theta_n, \theta_3, -\theta_2\}
 \tag{6}$$

$$\cos \theta_n = (1 - \theta_2^2 - \theta_3^2)^{1/2}
 \tag{7}$$

$$\theta_2 = -\frac{dw(s)}{ds}, \quad \theta_3 = \frac{dv(s)}{ds}
 \tag{8}$$

in which \mathbf{n} is the unit vector perpendicular to the vectors \mathbf{e}_1 and \mathbf{e}_1^S and \mathbf{t} is the tangent unit vector of the deformed centroid axis of the beam element. Note that \mathbf{e}_1^S coincides with \mathbf{t} . θ_n is the inverse of $\cos \theta_n$. $v(s)$ and $w(s)$ are the lateral deflections of the centroid axis of the beam element in the x_2 and x_3 directions, respectively, and s is the arc length of the deformed centroid axis.

Using Eqs. (2)–(8), the relation between the vectors \mathbf{e}_i and \mathbf{e}_i^S ($i = 1, 2, 3$) in the element coordinate system may be obtained as

$$\mathbf{e}_i^S = [\mathbf{t}, \mathbf{R}_1, \mathbf{R}_2] \mathbf{e}_i = \mathbf{R} \mathbf{e}_i
 \tag{9}$$

$$\begin{aligned}
 \mathbf{R}_1 &= \cos \theta_1 \mathbf{r}_1 + \sin \theta_1 \mathbf{r}_2, & \mathbf{R}_2 &= -\sin \theta_1 \mathbf{r}_1 + \cos \theta_1 \mathbf{r}_2 \\
 \mathbf{r}_1 &= \{-\theta_3, \cos \theta_n + (1 - \cos \theta_n)n_2^2, (1 - \cos \theta_n)n_2n_3\} \\
 \mathbf{r}_2 &= \{\theta_2, (1 - \cos \theta_n)n_2n_3, \cos \theta_n + (1 - \cos \theta_n)n_3^2\}
 \end{aligned}
 \tag{10}$$

where \mathbf{R} is the so-called rotation matrix. The rotation matrix is determined by θ_i ($i = 1, 2, 3$). Thus, θ_i are called rotation parameters in this study.

Let $\boldsymbol{\theta} = \{\theta_1, \theta_2, \theta_3\}$ be the column matrix of rotation parameters, $\delta\boldsymbol{\theta}$ be the variation of $\boldsymbol{\theta}$. The triad \mathbf{e}_i^S ($i = 1, 2, 3$) corresponding to $\boldsymbol{\theta}$ may be rotated by a rotation vector $\delta\boldsymbol{\phi} = \{\delta\phi_1, \delta\phi_2, \delta\phi_3\}$ to reach their new positions corresponding to $\boldsymbol{\theta} + \delta\boldsymbol{\theta}$ [16]. When θ_2 and θ_3 are much smaller than unity, the relationship between $\delta\boldsymbol{\theta}$ and $\delta\boldsymbol{\phi}$ may be approximated by [16]

$$\delta\boldsymbol{\theta} = \begin{bmatrix} 1 & \theta_3/2 & -\theta_2/2 \\ -\theta_3 & 1 & 0 \\ \theta_2 & 0 & 1 \end{bmatrix} \delta\boldsymbol{\phi} = \mathbf{T}^{-1} \delta\boldsymbol{\phi}.
 \tag{11}$$

2.4. Nodal parameters and forces

The element employed here has two nodes with six degrees of freedom per node. Two sets of element nodal parameters termed ‘explicit nodal parameters’ and ‘implicit nodal parameters’ are employed. The explicit nodal parameters of the element are used for the assembly of the system equations from the element equations. They are chosen to be u_{ij} , the x_i ($i = 1, 2, 3$) components of the translation vectors \mathbf{u}_j at node j ($j = 1, 2$) and ϕ_{ij} , the x_i ($i = 1, 2, 3$) components of the rotation vectors $\boldsymbol{\phi}_j$ at node j ($j = 1, 2$). Here, the values of $\boldsymbol{\phi}_j$ are reset to zero at current configuration. Thus, $\delta\phi_{ij}$, the variation of ϕ_{ij} , represent infinitesimal rotations about the x_i axes [16], and the generalized nodal forces corresponding to $\delta\phi_{ij}$ are m_{ij} , the conventional moments about the x_i axes. The generalized nodal forces corresponding to δu_{ij} , the variation of u_{ij} , are f_{ij} , the forces in the x_i directions.

The implicit nodal parameters of the element are used to determine the deformation of the beam element. They are chosen to be u_{ij} , the x_i ($i = 1, 2, 3$) components of the translation vectors \mathbf{u}_j at node j ($j = 1, 2$) and θ_{ij} , the nodal values of the rotation parameters θ_i ($i = 1, 2, 3$) at node j ($j = 1, 2$). The generalized nodal forces corresponding to δu_{ij} and $\delta\theta_{ij}$ are f_{ij} and m_{ij}^θ , the forces in the x_i directions and the generalized moments, respectively. Note that m_{ij}^θ are not conventional moments, because $\delta\theta_{ij}$ are not infinitesimal rotations about the x_i axes at deformed state.

In view of Eq. (11), the relations between the variation of the implicit and explicit nodal parameters maybe expressed as

$$\delta\mathbf{q}_\theta = \begin{Bmatrix} \delta\mathbf{u}_1 \\ \delta\theta_1 \\ \delta\mathbf{u}_2 \\ \delta\theta_2 \end{Bmatrix} = \begin{bmatrix} \mathbf{I} & \mathbf{0} & \mathbf{0} & \mathbf{0} \\ \mathbf{0} & \mathbf{T}_1^{-1} & \mathbf{0} & \mathbf{0} \\ \mathbf{0} & \mathbf{0} & \mathbf{I} & \mathbf{0} \\ \mathbf{0} & \mathbf{0} & \mathbf{0} & \mathbf{T}_2^{-1} \end{bmatrix} \begin{Bmatrix} \delta\mathbf{u}_1 \\ \delta\boldsymbol{\phi}_1 \\ \delta\mathbf{u}_2 \\ \delta\boldsymbol{\phi}_2 \end{Bmatrix} = \mathbf{T}_{\theta\phi} \delta\mathbf{q} \tag{12}$$

where $\delta\mathbf{u}_j = \{\delta u_{1j}, \delta u_{2j}, \delta u_{3j}\}$, $\delta\boldsymbol{\theta}_j = \{\delta\theta_{1j}, \delta\theta_{2j}, \delta\theta_{3j}\}$ and $\delta\boldsymbol{\phi}_j = \{\delta\phi_{1j}, \delta\phi_{2j}, \delta\phi_{3j}\}$, ($j = 1, 2$); \mathbf{I} and $\mathbf{0}$ are the identity and zero matrices of order 3×3 , respectively; \mathbf{T}_j^{-1} ($j = 1, 2$) are nodal values of \mathbf{T}^{-1} given in Eq. (11).

Let $\mathbf{f} = \{\mathbf{f}_1, \mathbf{m}_1, \mathbf{f}_2, \mathbf{m}_2\}$, $\mathbf{f}_\theta = \{\mathbf{f}_1, \mathbf{m}_1^\theta, \mathbf{f}_2, \mathbf{m}_2^\theta\}$, where $\mathbf{f}_j = \{f_{1j}, f_{2j}, f_{3j}\}$, $\mathbf{m}_j = \{m_{1j}, m_{2j}, m_{3j}\}$, and $\mathbf{m}_j^\theta = \{m_{1j}^\theta, m_{2j}^\theta, m_{3j}^\theta\}$ ($j = 1, 2$), denote the internal nodal force vectors corresponding to the variation of the explicit and implicit nodal parameters, $\delta\mathbf{q}$ and $\delta\mathbf{q}_\theta$, respectively. Using the contragradient law [18] and Eq. (12), the relation between \mathbf{f} and \mathbf{f}_θ , may be given by

$$\mathbf{f} = \mathbf{T}_{\theta\phi}^T \mathbf{f}_\theta \tag{13}$$

The global nodal parameters for the system of equations corresponding to the element local nodes j ($j = 1, 2$) should be consistent with the element explicit nodal parameters. Thus, they are chosen to be U_{ij} , the X_i ($i = 1, 2, 3$) components of the translation vectors \mathbf{U}_j at node j ($j = 1, 2$) and Φ_{ij} , the X_i ($i = 1, 2, 3$) components of the rotation vectors $\boldsymbol{\Phi}_j$ at nodes j ($j = 1, 2$). Here, the values of $\boldsymbol{\Phi}_j$ are reset to zero at current configuration. Thus, $\delta\Phi_{ij}$, the variation of Φ_{ij} , represent infinitesimal rotations about the X_i axes [16], and the generalized nodal forces corresponding to $\delta\Phi_{ij}$ are the conventional moments about the X_i axes. The generalized nodal forces corresponding to δU_{ij} , the variation of U_{ij} , are the forces in the X_i directions.

2.5. Kinematics of beam element

The deformations of the beam element are described in the current element coordinate system. From the kinematic assumptions made in this paper, the deformations of the beam element may be determined by the displacements of the centroid axis of the beam element, orientation of the cross section (element cross section coordinates), and the out-of-plane warping of the cross section. Let Q (Fig. 1) be an arbitrary point in the beam element, and P be the point corresponding to Q on the centroid axis. The position vector of point Q in the undeformed and deformed configurations may be expressed as

$$\mathbf{r}_0 = x\mathbf{e}_1 + y\mathbf{e}_2 + z\mathbf{e}_3 \tag{14}$$

and

$$\mathbf{r} = x_c(s)\mathbf{e}_1 + v(s)\mathbf{e}_2 + w(s)\mathbf{e}_3 + \theta_{1,s}\mathbf{e}_1^s + y\mathbf{e}_2^s + z\mathbf{e}_3^s \tag{15}$$

where $x_c(s)$, $v(s)$ and $w(s)$ are the x_1 , x_2 and x_3 coordinates of point P , respectively, s is the arc length of the deformed centroid axis measured from node 1 to point P . The relationship among $x_c(s)$, $v(s)$, $w(s)$ and s may be given as

$$x_c(s) = u_{11} + \int_0^s \cos \theta_n \, ds \tag{16}$$

where u_{11} is the displacement of node 1 in the x_1 direction, and $\cos \theta_n$ is defined in Eq. (7). Note that due to the definition of the element coordinate system, the value of u_{11} is equal to zero. However, the variation of u_{11} is not zero. Making use of Eq. (16), one obtains

$$S = \frac{2\ell}{\int_{-1}^1 \cos \theta_n \, d\xi} \tag{17}$$

$$\ell = x_c(S) - x_c(0) = L - u_{11} + u_{22} \tag{18}$$

and

$$\xi = -1 + \frac{2s}{S} \tag{19}$$

in which S and ℓ are the current arc length and chord length of the centroid axis of the beam element, respectively, and L is the chord length of the undeformed beam axis.

Here, the lateral deflections of the centroid axis $v(s)$ and $w(s)$ are assumed to be the Hermitian polynomials of s , and the rotation about the centroid axis $\theta_1(s)$ (Eq. (3)) is assumed to be linear polynomials of s . $v(s)$, $w(s)$ and $\theta_1(s)$ may be expressed by

$$\begin{aligned} v(s) &= \{N_1, N_2, N_3, N_4\}^t \{u_{21}, \theta_{31}, u_{22}, \theta_{32}\} = N_b^t \mathbf{u}_b \\ w(s) &= \{N_1, -N_2, N_3, -N_4\}^t \{u_{31}, \theta_{21}, u_{32}, \theta_{22}\} = N_c^t \mathbf{u}_c \\ \theta_1(s) &= \{N_5, N_6\}^t \{\theta_{11}, \theta_{12}\} = N_d^t \mathbf{u}_d \end{aligned} \tag{20}$$

where u_{2j} and u_{3j} ($j = 1, 2$) are nodal values of v and w at nodes j , respectively, and θ_{ij} ($i = 1, 2, 3, j = 1, 2$) are nodal values of θ_i at nodes j . Note that, due to the definition of the element coordinates, the values of u_{2j} and u_{3j} ($j = 1, 2$) are zero. However, their variations are not zero. N_i ($i = 1-6$) are shape functions and are given by

$$\begin{aligned} N_1 &= \frac{1}{4} (1 - \xi)^2 (2 + \xi), & N_2 &= \frac{S}{8} (1 - \xi^2) (1 - \xi), \\ N_3 &= \frac{1}{4} (1 + \xi)^2 (2 - \xi), & N_4 &= \frac{S}{8} (-1 + \xi^2) (1 + \xi), \\ N_5 &= \frac{1}{2} (1 - \xi), & N_6 &= \frac{1}{2} (1 + \xi). \end{aligned} \tag{21}$$

The axial displacements of the centroid axis may be determined from the lateral deflections and the unit extension of the centroid axis using Eq. (16).

If x , y and z in Eq. (14) are regarded as the Lagrangian coordinates, the Green strain ϵ_{11} , ϵ_{12} and ϵ_{13} are given by [19]

$$\begin{aligned} \epsilon_{11} &= \frac{1}{2} (\mathbf{r}_{,x}^t \mathbf{r}_{,x} - 1) \\ \epsilon_{12} &= \frac{1}{2} \mathbf{r}_{,x}^t \mathbf{r}_{,y} \\ \epsilon_{13} &= \frac{1}{2} \mathbf{r}_{,x}^t \mathbf{r}_{,z} \end{aligned} \tag{22}$$

Using the chain rule for differentiation, $\mathbf{r}_{,x}$ in Eq. (22) may be expressed as

$$\mathbf{r}_{,x} = \mathbf{r}_{,s} (1 + \epsilon_0) \tag{23}$$

$$\varepsilon_0 = \frac{\partial s}{\partial x} - 1 \quad (24)$$

where ε_0 is the unit extension of the centroid axis. Making use of the assumption of uniform unit extension, one may rewrite Eq. (24) as

$$\varepsilon_0 = \frac{S}{L} - 1. \quad (25)$$

Substituting Eqs. (5)–(10), (15), (23), (25) into Eq. (22), ε_{11} , ε_{12} and ε_{13} can be calculated. ε_{11} , ε_{12} and ε_{13} are given in [16] and are not repeated here.

2.6. Element nodal force vector

The element nodal force vector \mathbf{f}_θ (Eq. (13)) corresponding to the implicit nodal parameters are obtained from the virtual work principle in the current element coordinates. It should be mentioned again that *the element coordinate system is a local coordinate system not a moving coordinate system*. Thus, a standard procedure is used here for the derivation of \mathbf{f}_θ . For convenience, the implicit nodal parameters are divided into four generalized nodal displacement vectors \mathbf{u}_i ($i = a, b, c, d$), where

$$\mathbf{u}_a = \{u_{11}, u_{12}\} \quad (26)$$

and \mathbf{u}_b , \mathbf{u}_c and \mathbf{u}_d are defined in Eq. (20).

The generalized force vectors corresponding to $\delta\mathbf{u}_i$, the variation of \mathbf{u}_i ($i = a, b, c, d$) are

$$\begin{aligned} \mathbf{f}_a &= \{f_{11}, f_{12}\} \\ \mathbf{f}_b &= \{f_{21}, m_{31}^\theta, f_{22}, m_{32}^\theta\} \\ \mathbf{f}_c &= \{f_{31}, m_{21}^\theta, f_{32}, m_{22}^\theta\} \\ \mathbf{f}_d &= \{m_{11}^\theta, m_{12}^\theta\}. \end{aligned} \quad (27)$$

The virtual work principle requires that

$$\begin{aligned} \delta\mathbf{u}_a^t \mathbf{f}_a + \delta\mathbf{u}_b^t \mathbf{f}_b + \delta\mathbf{u}_c^t \mathbf{f}_c + \delta\mathbf{u}_d^t \mathbf{f}_d \\ = \int_V (\sigma_{11} \delta\varepsilon_{11} + 2\sigma_{12} \delta\varepsilon_{12} + 2\sigma_{13} \delta\varepsilon_{13}) dV \end{aligned} \quad (28)$$

where V is the volume of the undeformed beam, $\sigma_{11} = E\varepsilon_{11}$, $\sigma_{12} = 2G\varepsilon_{12}$, and $\sigma_{13} = 2G\varepsilon_{13}$, where E is the Young's modulus and G is shear modulus.

If the element size is chosen small enough, the values of the nodal parameters (displacements and rotation parameters) of the element defined in the current element coordinate system may always be much smaller than unity. Thus, the higher-order terms of nodal parameters in the element internal nodal forces may be neglected. However, in order to include the nonlinear coupling among the bending, twisting, and stretching deformations, the terms up to the second order of nodal parameters are retained in element internal nodal forces by consistent linearization of Eq. (28). The nodal force vectors \mathbf{f}_i ($i = a, b, c, d$) are given in [16] and not repeated here.

2.7. Element tangent stiffness matrices

The element tangent stiffness matrix corresponding to the explicit nodal parameters (referred to as explicit tangent stiffness matrix) may be obtained by differentiating the element nodal force vector \mathbf{f} in Eq. (13) with respect to explicit nodal parameters. Using Eqs. (12) and (13), we obtain

$$\mathbf{k} = \frac{\partial \mathbf{f}}{\partial \mathbf{q}} = \frac{\partial \mathbf{f}}{\partial \mathbf{q}_\theta} \frac{\partial \mathbf{q}_\theta}{\partial \mathbf{q}} = \mathbf{T}_{\theta d}^T \mathbf{k}_\theta \mathbf{T}_{\theta \phi} + \mathbf{H} \quad (29)$$

where $\mathbf{k}_\theta = \partial \mathbf{f}_\theta / \partial \mathbf{q}_\theta$ is the tangent stiffness matrix corresponding to implicit nodal parameters (referred to as implicit tangent stiffness matrix), and \mathbf{H} is a unsymmetrical matrix and is given by

$$H = \begin{bmatrix} \mathbf{0} & \mathbf{0} & \mathbf{0} & \mathbf{0} \\ \mathbf{0} & H_1 & \mathbf{0} & \mathbf{0} \\ \mathbf{0} & \mathbf{0} & \mathbf{0} & \mathbf{0} \\ \mathbf{0} & \mathbf{0} & \mathbf{0} & H_2 \end{bmatrix} \tag{30}$$

in which $\mathbf{0}$ is a zero matrix of order 3×3 and

$$H_j = \begin{bmatrix} 0 & m_{3j}^\theta & -m_{2j}^\theta \\ 0 & 0 & \frac{1}{2} m_{1j}^\theta \\ 0 & -\frac{1}{2} m_{1j}^\theta & 0 \end{bmatrix}. \tag{31}$$

Using the direct stiffness method, the implicit tangent stiffness matrix k_θ may be assembled by the submatrices

$$k_{ij} = \frac{\partial f_i}{\partial u_j} \tag{32}$$

where f_i ($i = a, b, c, d$) are defined in Eq. (27) and u_i ($i = a, b, c, d$) are defined in Eqs. (20) and (26). k_{ij} are given in [16], and are not repeated here. It is noted that the element tangent stiffness matrix k in Eq. (29) is unsymmetrical. This observation is consistent with that of Simo and Vu-Quoc [20] and Crisfield [21] who adopted different formulation. However, numerical experiments of the present authors have shown that for conservative problems the tangent stiffness matrix of the structure become symmetrical at equilibrium configuration. This observation is again consistent with the theory of Simo and Vu-Quoc.

Note that because only the terms up to the second order of nodal parameters are retained in f_θ , only the terms up to the first order of nodal parameters are retained in the element stiffness matrix given in Eq. (29). Thus the element stiffness matrix in Eq. (29) may be rewritten symbolically as

$$k = k_0 + k_1 \tag{33}$$

where k_0 comprises all zeroth order terms of nodal parameters in k and k_1 comprises all first-order terms of nodal parameters in k . k_0 is the linear stiffness matrix of elementary beam element, and k_1 is the geometrical stiffness matrix.

Note that the element coordinate system is only a local coordinate system not a moving or rotating coordinate system here. Thus, the element tangent stiffness matrix referred to the global coordinate system is obtained by using the standard coordinate transformation and may be expressed by

$$k^G = T_{GE} k T_{GE}^t \tag{34}$$

$$T_{GE} = \begin{bmatrix} A_{GE} & \mathbf{0} & \mathbf{0} & \mathbf{0} \\ \mathbf{0} & A_{GE} & \mathbf{0} & \mathbf{0} \\ \mathbf{0} & \mathbf{0} & A_{GE} & \mathbf{0} \\ \mathbf{0} & \mathbf{0} & \mathbf{0} & A_{GE} \end{bmatrix} \tag{35}$$

where $\mathbf{0}$ is a zero matrix of order 3×3 and A_{GE} is defined in Eq. (1).

2.8. Load stiffness matrix

Different ways for generating configuration dependent moment were proposed in the literature [5,6]. Here, for simplicity, only the conservative moments generated by conservative force or forces (with fixed directions) are considered, and two possible ways for generating conservative moment are employed. In this study, a set of load base coordinates X_i^P ($i = 1, 2, 3$) associated with each configuration dependent moment are constructed at the current configuration. The mechanism for generating configuration dependent moment is described in this coordinates, and the corresponding external load and load stiffness matrix [22] are defined in terms of this coordinates. Unless stated otherwise, all vectors and matrices in this section are referred to this coordinates. Note that this coordinate system is just a local coordinate system constructed at the current configuration, not a

moving coordinate system. Thus, it is regarded as a fixed coordinated system in the derivation of the load stiffness matrix.

The first way for generating configuration dependent moment may be described as follows.

Consider a sphere of radius R which centroid is rigidly connected with the structure at node O as shown in Fig. 3. Two strings wound around a great circle of the sphere are acted upon by forces of magnitude P . Thus, the strings are always tangent to the sphere. The great circle and the forces are on the same plane at the undeformed configuration of the structure. However, the great circle and the forces are generally not on the same plane when the structure is deformed. The origin of the load base coordinate system is chosen to be located at the node O . The X_1^P axis is chosen to coincide with the normal of the plane of the great circle, and the X_2^P and X_3^P axes lie in the plane of the great circle.

Let A denote the contact point of the force P and the great circle. Because P is tangent to the sphere, P is perpendicular to the line OA . Let e_A denote unit vector in the direction of line OA . e_A may be expressed by

$$e_A = a / (a^T a)^{1/2} \tag{36}$$

$$a = e_p^P \times n^P = \{0, \ell_3, -\ell_2\} \tag{37}$$

where $e_p^P = \{\ell_1, \ell_2, \ell_3\}$ is the unit vector in the direction of P , and n^P is the unit normal of the plane of the great circle. Note that n^P coincides with $e_1^P = \{1, 0, 0\}$, the unit vector associated with the X_1^P axis.

The external moment vector at node O generated by the above mentioned mechanism may be expressed by

$$M = M e_A \times e_p^P \tag{38}$$

where $M = 2RP$ is the magnitude of the moment.

The moment in Eq. (38) is rotation dependent. When an incremental rotation vector $\Delta\varphi^P = \{\Delta\varphi_1, \Delta\varphi_2, \Delta\varphi_3\}$ passing through node O is applied to the sphere, the unit normal of the plane of the great circle, n^P has an incremental change Δn^P . If the magnitude of $\Delta\varphi^P$ is small enough, Δn^P may be expressed as

$$\Delta n^P = \Delta\varphi^P \times n^P = \{0, \Delta\varphi_3, -\Delta\varphi_2\}. \tag{39}$$

Note that $\Delta\varphi^P$ is not applied to the load base coordinates here. The incremental moment corresponding to $\Delta\varphi^P$ may be expressed by

$$\Delta M = M \Delta e_A \times e_p^P \tag{40}$$

where

$$\Delta e_A = \frac{1}{(a^T a)^{1/2}} \Delta a \times e_p^P - \frac{a^T \Delta a}{(a^T a)^{3/2}} a \times e_p^P \tag{41}$$

$$\Delta a = e_p^P \times \Delta n^P \tag{42}$$

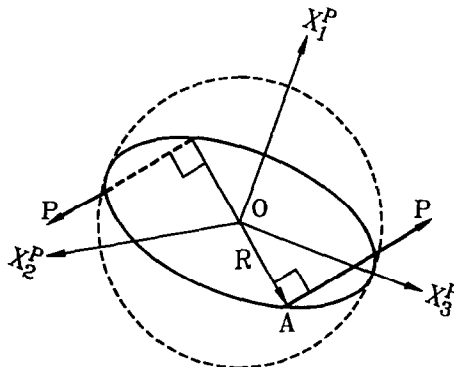


Fig. 3. Mechanism for generating configuration dependent moment.

Using the tangent stiffness approach, the relation between the incremental moment ΔM and the corresponding load stiffness matrix k_p may be expressed as

$$\Delta M = k_p \Delta \varphi^P. \tag{43}$$

From Eqs. (36), (37), and (39)–(43), one obtains

$$k_p = M(\ell_2^2 + \ell_3^2)^{-1/2} k_{pa} + M(\ell_2^2 + \ell_3^2)^{-3/2} k_{pb} \tag{44}$$

where

$$k_{pa} = \begin{bmatrix} 0 & \ell_1 \ell_3 & -\ell_1 \ell_2 \\ 0 & \ell_2 \ell_3 & \ell_1^2 + \ell_3^2 \\ 0 & -\ell_1^2 - \ell_2^2 & -\ell_2 \ell_3 \end{bmatrix} \tag{45}$$

$$k_{pb} = \begin{bmatrix} 0 & -\ell_1 \ell_3 (\ell_2^2 + \ell_3^2) & \ell_1 \ell_2 (\ell_2^2 + \ell_3^2) \\ 0 & \ell_1^2 \ell_2 \ell_3 & -\ell_1^2 \ell_2^2 \\ 0 & \ell_1^2 \ell_3^2 & -\ell_1^2 \ell_2 \ell_3 \end{bmatrix} \tag{46}$$

Three special cases shown in Fig. 4 are considered here. Following [5], they are referred to as quasitangential (QT) moments of the first and second type, and semitangential (ST) moment. The load stiffness matrices corresponding to QT and ST moment at the configurations shown in Fig. 4 may be obtained from Eqs. (44)–(46) and given by

$$k_p^{QT1} = M \begin{bmatrix} 0 & 0 & 0 \\ 0 & 0 & 0 \\ 0 & -1 & 0 \end{bmatrix} \tag{47}$$

$$k_p^{QT2} = M \begin{bmatrix} 0 & 0 & 0 \\ 0 & 0 & 1 \\ 0 & 0 & 0 \end{bmatrix} \tag{48}$$

$$k_p^{ST} = \frac{M}{2} \begin{bmatrix} 0 & 0 & 0 \\ 0 & 0 & 1 \\ 0 & -1 & 0 \end{bmatrix}. \tag{49}$$

The second way for generating configuration dependent moment may be described as follows.

Consider a rigid arm of length R which end is rigidly connected with the structure at node O as shown in Fig. 5. The other end of the rigid arm is acted upon by a conservative force (with a fixed direction) of magnitude P . The origin of the load base coordinates X_i^P ($i = 1, 2, 3$) is chosen to be located at the node O . The X_1^P axis is chosen to coincide with the axis of the rigid arm, and the X_2^P and X_3^P axes are perpendicular to the rigid arm.

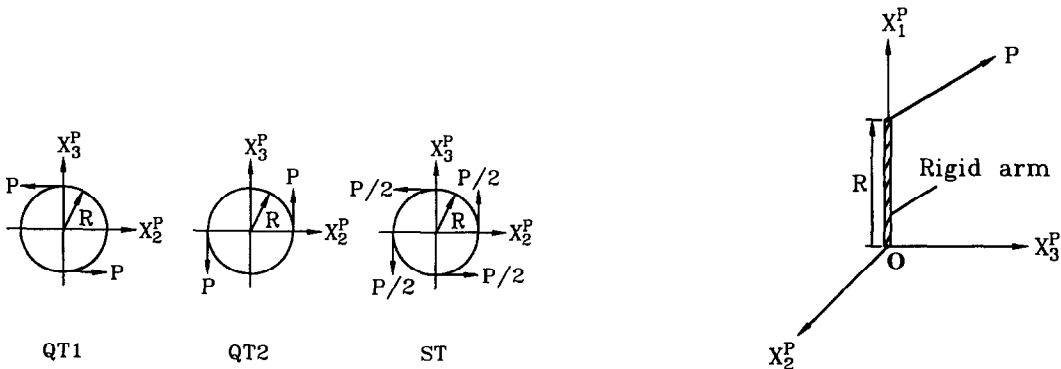


Fig. 4. Quasitangential (QT) moment and semitangential (ST) moment.

Fig. 5. Mechanism for generating configuration dependent moment by an off-axis load.

The external moment vector at node O generated by the above mentioned mechanism may be expressed by

$$\mathbf{M} = R\mathbf{P}t^P \times \mathbf{e}_p^P \tag{50}$$

where $\mathbf{e}_p^P = \{\ell_1, \ell_2, \ell_3\}$ is the unit vector in the direction of \mathbf{P} and t^P is the unit vector in the axial direction of the rigid arm. Note that t^P coincides with $\mathbf{e}_1^P = \{1, 0, 0\}$, the unit vector associated with the X_1^P axis.

The moment in Eq. (50) is rotation dependent. When an incremental rotation vector $\Delta\boldsymbol{\varphi}^P = \{\Delta\varphi_1, \Delta\varphi_2, \Delta\varphi_3\}$ passing through node O is applied to the rigid arm, the unit vector t^P has an incremental change Δt^P . If the magnitude of $\Delta\boldsymbol{\varphi}^P$ is small enough, Δt^P may be expressed as

$$\Delta t^P = \Delta\boldsymbol{\varphi}^P \times t^P = \{0, \Delta\varphi_3, -\Delta\varphi_2\}. \tag{51}$$

Note that $\Delta\boldsymbol{\varphi}^P$ is not applied to the load base coordinates here. The incremental moment corresponding to $\Delta\boldsymbol{\varphi}^P$ may be expressed by

$$\begin{aligned} \Delta\mathbf{M} &= M \Delta t^P \times \mathbf{e}_p^P \\ &= RP\{\ell_2 \Delta\varphi_2 + \ell_3 \Delta\varphi_3, -\ell_1 \Delta\varphi_2, -\ell_1 \Delta\varphi_3\}. \end{aligned} \tag{52}$$

From Eqs. (43) and (52), the corresponding load stiffness matrix may be expressed as

$$\mathbf{k}_p = RP \begin{bmatrix} 0 & \ell_2 & \ell_3 \\ 0 & -\ell_1 & 0 \\ 0 & 0 & -\ell_1 \end{bmatrix}. \tag{53}$$

The load stiffness matrix referred to the global coordinate system is obtained by using the standard coordinate transformation and may be expressed by

$$\mathbf{k}_p^G = \mathbf{A}_{GP} \mathbf{k}_p \mathbf{A}_{GP}^T \tag{54}$$

where \mathbf{A}_{GP} is the transformation matrix given in Eq. (1).

3. Consistent linear buckling analysis

3.1. Assumptions

Four assumptions are made in the present buckling analysis and given as follows:

- (1) The external loading is proportional to one loading parameter.
- (2) The prebuckling displacements and rotations of the structure and the corresponding deformations and rigid body rotations of the beam element are linearly proportional to the external loading.
- (3) The prebuckling rotations of the structure are rotations about axes with the same fixed direction or small rotations.
- (4) The effect of the prebuckling displacements on the transformation matrix for coordinate transformation may be ignored.

3.2. Criterion of the buckling state

Here, the zero value of the tangent stiffness matrix determinant is used as the criterion of the buckling state. Let $\mathbf{K}_T(\lambda)$ denote the tangent stiffness matrix of the structure corresponding to the loading parameter λ . The criterion of the buckling state may be expressed as

$$D(\lambda) = \det|\mathbf{K}_T(\lambda)| = 0. \tag{55}$$

The minimum root of Eq. (55) is the buckling load.

3.3. Determination of the tangent stiffness matrix of the structure

The tangent stiffness matrix of the structure corresponding to λ is assembled by the element stiffness matrices and load stiffness matrices corresponding to λ using direct stiffness method. The element tangent stiffness matrix corresponding to λ may be determined as follows.

A linear analysis for $\lambda = 1$ is carried out first. Let $\mathbf{u}_j^L = \{u_{1j}^L, u_{3j}^L, u_{3j}^L\}$ and $\boldsymbol{\phi}_j^L = \{\phi_{1j}^L, \phi_{3j}^L, \phi_{3j}^L\}$ ($j = 1, 2$) (referred to the initial element coordinates) denote displacement and rotation vectors of an element at node j , which are extracted from the linear solution for $\lambda = 1$, and then transformed from the global coordinates to the initial element coordinates. The rotation vector corresponding to rotation about axis with fixed direction or small rotation may be regarded as true vector. Thus, making use of assumptions (2) and (3), the rigid body rotation vector of the element $\boldsymbol{\phi}^R$ and the vectors of the deformational rotation parameters $\boldsymbol{\theta}_j$ at nodes j ($j = 1, 2$) corresponding to \mathbf{u}_j^L and $\boldsymbol{\phi}_j^L$ ($j = 1, 2$) may be determined by

$$\boldsymbol{\phi}^R = \left\{ \frac{1}{2} (\phi_{11}^L + \phi_{12}^L), -\frac{1}{L} (u_{32}^L - u_{31}^L), \frac{1}{L} (u_{22}^L - u_{21}^L) \right\} \quad (56)$$

$$\boldsymbol{\theta}_j = \boldsymbol{\phi}_j^R - \boldsymbol{\phi}^R \quad (57)$$

where L is the initial length of the beam element. The unit extension of the centroid axis of the beam element may be determined by

$$\varepsilon_0 = \frac{1}{L} (u_{12}^L - u_{11}^L). \quad (58)$$

Making use of assumption (2), and Eqs. (56)–(58), the element tangent stiffness matrix given in Eq. (33) corresponding to loading parameter λ referred to the current element coordinates can be calculated and written in the form

$$\mathbf{k} = \mathbf{k}_0 + \lambda \mathbf{k}_1^{\text{ref}} \quad (59)$$

where $\mathbf{k}_1^{\text{ref}}$ is the geometric stiffness matrix corresponding to $\lambda = 1$.

The current element coordinates corresponding to loading parameter λ can be obtained by the application of the rotation vector $\lambda \boldsymbol{\phi}^R$ to the initial element coordinates. The current load base coordinates corresponding to loading parameter λ can be obtained by the application of the rotation vector $\lambda \boldsymbol{\phi}_p^L$ to the initial load base coordinates, where $\boldsymbol{\phi}_p^L$ is the rotation vector at the origin of the load base coordinates, which is extracted from the linear solution for $\lambda = 1$. However, making use of assumption (4), the initial transformation matrices \mathbf{A}_{GE} and \mathbf{A}_{GP} constructed at the undeformed structure are used in Eqs. (34) and (54), respectively, for different values of loading parameter λ . Thus, the tangent stiffness matrix of the structure is also a linear function of the loading parameter λ , and may be written in the form

$$\mathbf{K}_T = \mathbf{K}_0 + \lambda \mathbf{K}_1^{\text{ref}} \quad (60)$$

where \mathbf{K}_0 is the linear stiffness matrix of the structure, and $\mathbf{K}_1^{\text{ref}}$ is the geometric stiffness matrix of the structure corresponding to $\lambda = 1$.

3.4. Calculation of the buckling load

From Eq. (60), we know that Eq. (55) is equivalent to the generalized eigenvalue problem

$$\mathbf{K}_0 \mathbf{Q} = -\lambda \mathbf{K}_1^{\text{ref}} \mathbf{Q} \quad (61)$$

where \mathbf{Q} is the eigenvector. The minimum eigenvalue of Eq. (61) is the buckling load and the corresponding eigenvalue is the buckling mode. Here, the inverse power method [23] is used to find the buckling load and buckling mode.

4. Numerical studies

EXAMPLE 4.1: *Cantilever beam subjected to end force.* The example considered here is a cantilever beam subjected to a lateral end force P as shown in Fig. 6. The X_i^G ($i = 1, 2, 3$) axes of the global coordinate system shown in Fig. 6 coincide with x_i^S axes, the axes of the element cross section coordinate system in the undeformed beam. The geometry and material properties are: length $L = 1$ m, cross sectional area $A = 3 \times 10^{-5}$ m, moment of inertia about x_2^S axis $I_y = 1.25 \times 10^{-9}$ m⁴, moment of inertia about x_3^S axis $I_z = 10^{-8}$ m⁴, torsional constant $J = 10^{-10}$ m⁴, Young’s modulus $E = 1.0 \times 10^8$ N/m², and shear modulus $G = 5 \times 10^7$ N/m². The classical buckling load for this example is $P_{cr} = (4.013/L^2)\sqrt{EI_y GJ} = 0.10033$ N [3].

The buckling loads of the present study together with the results of [6] and [12] are given in Table 1. Very good agreement among all these solutions is observed.

EXAMPLE 4.2: *Cantilever beam subjected to end moment.* The example considered here is a cantilever beam subjected to end moment M . The quasitangential and semitangential moments are considered. The corresponding load base coordinates are shown in Fig. 7. The geometry and material properties of the beam are identical with those of Example 1. The classical buckling moment is quoted in [3] as

$$M_{cr} = \begin{cases} \frac{\pi}{2L} \sqrt{EI_y GJ} & \text{for QT} \\ \frac{\pi}{L} \sqrt{EI_y GJ} & \text{for ST} \end{cases}$$

The buckling loads of the present study together with the finite element results of [6] and [12], and analytical solution of [3] are given in Table 2. The results of the present study, [6], and [12] are obtained using ten elements. Very good agreement among all these solutions is observed.

EXAMPLE 3: *Cantilever angle subjected to a horizontal end force.* The example of the end cross section as shown in Fig. 8. Here $P(+)$ and $P(-)$ denote forces directed along positive and negative X_1^G axis, respectively. The geometry and material properties are: $L = 240$ mm, $b = 0.6$ mm, $h = 30$ mm, Young’s modulus $E = 71240$ N/mm², and shear modulus $G = 27191$ N/mm².

The buckling loads of the present study obtained by using 20 elements for $P(+)$ and $P(-)$ are 1.0880 N and 0.6804 N, respectively. The results of the present study are identical with those results given by Argyris et al. [7] using 20 elements.

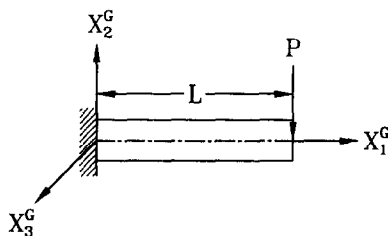


Fig. 6. Cantilever beam subjected to lateral load.

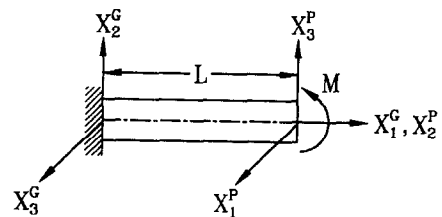


Fig. 7. Cantilever beam subjected to end moment.

Table 1
Critical load of cantilever beam subjected to end force

Number of elements	Critical loads P_{cr} (N)		
	Present	Argyris [6]	Saleeb [12]
2	0.10317	0.107251	0.1414
4	0.10061	0.101857	0.1083
6	0.10043	0.101002	0.1037
10	0.10036	0.100536	0.1016

Table 2
Critical load of cantilever beam subjected to end moment

	Critical moments M_{cr} (N · cm)	
	QT1 and QT2	ST
Present	3.929	7.868
Argyris [7]	3.93103	7.88632
Saleeb [12]	3.9348	7.9170
Theory [3]	3.927	7.854

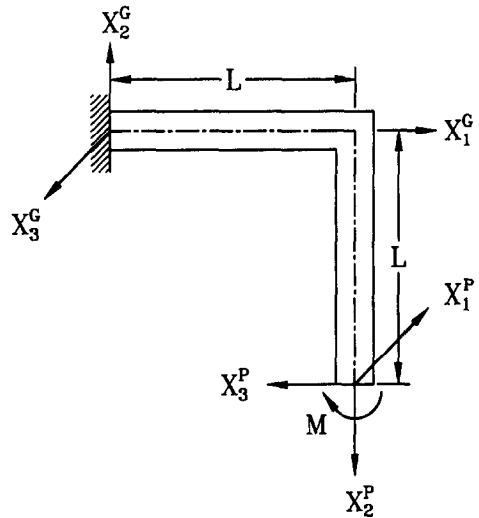
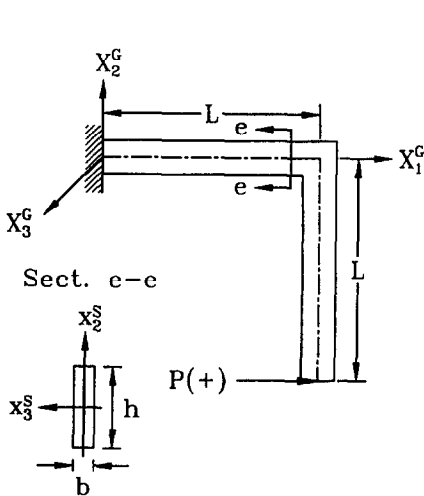


Fig. 8. Cantilever angle subjected to a horizontal end force.

Fig. 9. Cantilever angle subjected to end moment.

EXAMPLE 4: Cantilever angle subjected to end moment. The example considered here is a cantilever angle subjected to end moment M . The quasitangential and semitangential moments are considered. The corresponding load base coordinates are shown in Fig. 9. The geometry and material properties of the beam are identical with those of Example 1.

The buckling moments of the present study together with the results of [6] and [12] are given in Table 3. Very good agreement among all these solutions is observed.

Table 3
Critical moments for cantilever angle with end bending moment

Type of moment	Number of elements	Critical moments M_{cr} (N · cm)		
		Present	Argyris [6]	Salceeb [12]
QT1	8	0.4934	0.4935	0.4936
	12	0.4935	0.4935	0.4935
	20	0.4935	0.4935	0.4935
QT2	8	3.445	3.453	3.467
	12	3.439	3.442	3.448
	20	3.435	3.437	3.439
ST	8	0.98655	0.98699	0.9878
	12	0.98679	0.98698	0.9873
	20	0.98691	0.98698	0.9871

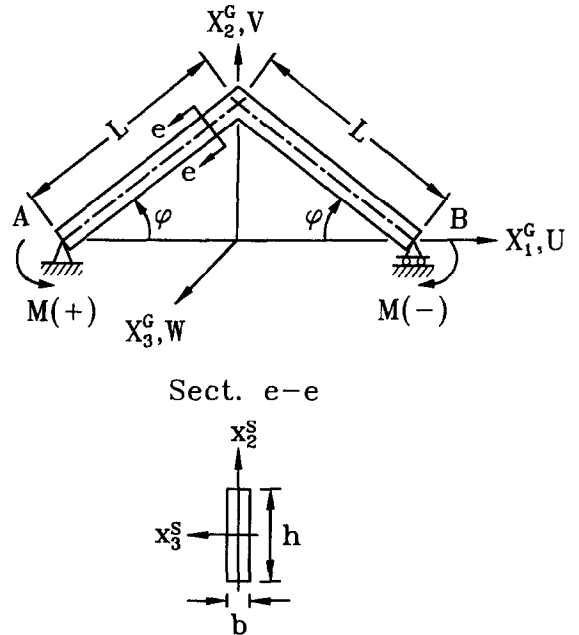
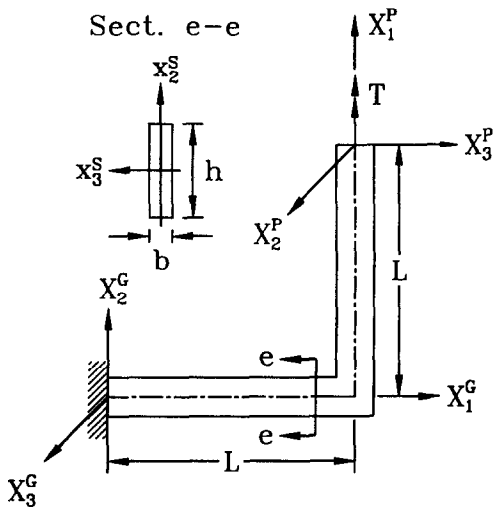


Fig. 10. Cantilever angle subjected to end torsion.

Fig. 11. Simply supported angle frame subjected to uniform moment.

EXAMPLE 5: Cantilever angle subjected to end torsion. The example considered here is a cantilever angle subjected to end torsion T . The quasitangential and semitangential moments are considered. The corresponding load base coordinates are shown in Fig. 10. Two cases of cross section are considered: (1) $b = 0.6$ mm, $h = 10$ mm, (2) $b = 10$ mm, $h = 0.6$ mm. The rest geometry and material properties of the angle are: $L = 240$ mm, Young's modulus $E = 71240$ N/mm², and shear modulus $G = 27191$ N/mm².

The present results obtained by using 80 elements are shown in Table 4 together with the results of [10]. As can be seen, the discrepancy between these two results are remarked for case (1) is observed. Note that the prebuckling displacements for this example is quite large. Thus a nonlinear buckling analysis [6,24,25] may be required for reliable solutions.

EXAMPLE 6: Simply supported angle frame subjected to uniform moment. The example considered here is a simply supported angle frame subjected to uniform moment M as shown in Fig. 11. Here, $M(+)$ and $M(-)$ denote moments about positive and negative X_3^G axis, respectively. The ends of the beam are free to rotate about X_3^G axis, but rotation about X_1^G and X_2^G axes are prevented. The translation of end point A is restrained, and end points B is free to move in the direction of X_1^G axis. Because of the rotational boundary conditions used here, the ways of generating end moments are rendered irrelevant here. The geometry and material properties are identical with those of Example 3. The theoretical results is $M_{cr} = \pi/L\sqrt{EI_y GJ} = 622.21$ N·mm [3], which is independent of the angle ϕ shown in Fig. 11.

Table 4
Critical moment for cantilever with end torsion

Type of moment	Critical moment T_{cr} (N·mm)			
	$b \times h = 0.6$ mm \times 10 mm		$b \times h = 10$ mm \times 0.6 mm	
	Present	Yang [10]	Present	Yang [10]
QT1	262.2	833	56.6	60.6
QT2	271.1	729	103.1	106.1
ST	274.6	1444	112.4	110.4

The buckling moment of the present study and results given by [6] and [12] are 624.76, 624.77, and 627.37 N · mm, respectively, for $M(+/-)$ and $M(-/+)$ and different values of angle φ . All these results are obtained using 20 elements.

EXAMPLE 7: Simply supported beam subjected to a central concentrated load. The example considered here is a simply supported beam subjected to a concentrated load P at the middle as shown in Fig. 12. Here, three cases are considered for the application point of P : (1) upper face, (2) centroid and (3) lower face. The ends of the beam are free to rotate about X_2^G and X_3^G axes, but rotation about X_1^G axis is restrained. The translation is restrained at end point A, and is free only in the direction of X_1^G axis at points B. The geometry and material

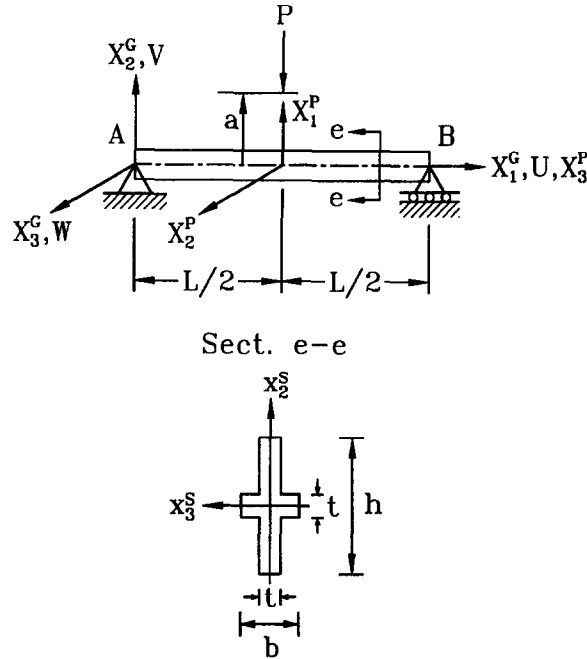


Fig. 12. Simply supported beam subjected to a central concentrated load.

Table 5
Critical loads for simply supported beam with central concentrated load

Load applied at	L (m)	P_{cr} (N)	P_{CLB}/P_{cr}^a
Upper face	1	2460.03	0.998
	2	740.37	1.396
	3	529.85	1.083
	4	354.51	1.025
	5	248.57	1.007
Centroid	1	8382.96	1.000
	2	2095.74	1.000
	3	931.44	1.000
	4	523.94	1.000
	5	335.32	1.000
Lower face	1	19225.96	0.888
	2	3451.12	1.013
	3	1333.03	1.029
	4	693.36	1.028
	5	422.06	1.025

^a P_{CLB} = Critical load of the present study.

properties are: $L = 1, 2, 3, 4, 5$ m, $b = 0.06$ m, $h = 0.1$ m, $t = 0.002$ m, Young's modulus $E = 2.04 \times 10^{11}$ N/m², and shear modulus $G = 7.9 \times 10^{10}$ N/m². The classical buckling moment is quoted in [3] as

$$P_{cr} = \frac{16.94\sqrt{EI_y GJ}}{L^2} \left(1 - \frac{1.74a}{L} \sqrt{\frac{EI_y}{GJ}} \right), \quad a = \begin{cases} 0.5 h & \text{for upper face} \\ 0 & \text{for centroid} \\ -0.5 h & \text{for lower face} \end{cases}$$

The present results obtained by using 40 elements are shown in Table 5 together with the analytical solution of [3]. As can be seen, when the load is applied at the centroid, the results of the present study are identical with those results given in [3]. When the load is applied at the upper face, the maximum discrepancy (39.6%) between these two results occurs at $L = 2$ m.

5. Conclusions

This paper has proposed a consistent linear buckling analysis of three-dimensional elastic Euler beams by using consistent second-order linearization of the fully geometrically nonlinear beam theory. The beam element proposed in [16] for nonlinear analysis is modified and employed here. All coupling among bending, twisting and stretching deformations for beam element is exactly considered by consistent linearization of the fully geometrically nonlinear beam theory. Based on the assumptions that the prebuckling displacements and rotations are linearly proportional to the external loading, the prebuckling rotations of the structure are fixed axis rotations or small rotations, and the effect of the prebuckling displacement on transformation matrix for the coordination can be ignored, a generalized eigenvalue problem is obtained for linear buckling analysis. An inverse power method for the solution of the generalized eigenvalue problem is used to find the buckling load and buckling mode. Numerical examples are presented to demonstrate the accuracy and efficiency of the proposed method. The agreement between the results of the present study and those given in the literature is very good for most examples. However, for some cases with large prebuckling displacements, the discrepancy between the results of the present study and classical solutions given in the literature is not small. Thus when the prebuckling displacements are not negligible, a nonlinear buckling analysis may be required for reliable solutions.

References

- [1] W.F. Chen and E.M. Lui, *Structural Stability, Theory and Implementation* (Elsevier Science Publishing Co., Inc. NY, 1988).
- [2] V.Z. Vlasov, *Thin Walled Elastic Beams*, 2nd edition (English translation published for U.S. Science Foundation by Israel Program for Scientific Translations, 1961).
- [3] S.P. Timoshenko and J.M. Gere, *Theory of Elastic Stability*, 2nd edition (McGraw-Hill, NY, 1963).
- [4] R.S. Barsoum and R.H. Gallagher, Finite element analysis of torsional and torsional-flexural stability problems, *Moments*, Int. J. Numer. Methods Engrg. 2 (1970) 335–352.
- [5] H. Ziegler, *Principles of Structural Stability* (Birkhauser, Verlag, Basel, 1977).
- [6] J.H. Argyris, P.C. Dunne and D.W. Scharpf, On large displacement-small strain analysis of structures with rotation degree of freedom, *Comput. Methods Appl. Mech. Engrg.* 14 (1978) 401–451; 15 (1978) 99–135.
- [7] J.H. Argyris, O. Hilpert, G.A. Malejannakis and D.W. Scharpf, On the geometrical stiffness of a beam in space—A consistent v.w. Approach, *Comput. Methods Appl. Mech. Engrg.* 20 (1979) 105–131.
- [8] J.H. Argyris, H. Balmer, J.St. Doltsinis, P.C. Dunne, M. Haase, M. Kleiber, G.A. Malejannakis, H.P. Mlejnek, M. Muller and D.W. Scharpf, *Finite Element Method—The natural approach*, *Comput. Methods Appl. Mech. Engrg.* 17/18 (1979) 1–106.
- [9] M.M. Attard, Lateral buckling analysis of beams by FEM, *Comput. Struct.* 23 (1986) 217–231.
- [10] Y.B. Yang and S.R. Kuo, Buckling of frames under various torsional loading, *J. Engrg. Mech.*, ASCE 117 (1991) 1681–1697.
- [11] Z.P. Bazant and L. Cedolin, *Stability of Structures* (Oxford University Press, 1991).
- [12] A.F. Saleeb, T.Y.P. Chang and A.S. Gendy, Effective modeling of spatial buckling of beam assemblages, accounting for warping constraints and rotation-dependency of moments, *Int. J. Numer. Methods Engrg.* 33 (1992) 469–502.
- [13] M.Y. Kim, S.P. Chang and S.B. Kim, Spatial stability analysis of thin walled space frames, *Int. J. Numer. Methods Engrg.* 39 (1996) 499–525.
- [14] J.C. Simo and L. Vu-Quoc, The role of non-linear theories in transient dynamic analysis of flexible structures, *J. Sound Vib.* 119 (1987) 487–508.
- [15] A.S. Gendy and A.F. Saleeb, Generalized mixed finite element model for pre- and post-quasistatic buckling response of thin-walled framed structures, *Int. J. Numer. Methods Engrg.* 37 (1994) 297–322.
- [16] K.M. Hsiao, Corotational total Lagrangian formulation for three-dimensional beam element, *AIAA J.* 30 (1992) 797–804.

- [17] H. Goldstein, *Classical Mechanics* (Addison-Wesley, Reading, MA, 1980).
- [18] D.J. Dawe, *Matrix and Finite Element Displacement Analysis of Structures* (Oxford University, NY, 1984).
- [19] T.J. Chung, *Continuum Mechanics* (Prentice-Hall Englewood Cliffs, NJ, 1988).
- [20] J.C. Simo and L. Vu-Quoc, A three-dimensional finite strain rod model. Part II: Computational aspects, *Comput. Methods Appl. Mech. Engrg.* 58 (1986) 79–116.
- [21] M.A. Crisfield, A consistent co-rotational formulation for non-linear, three-dimensional, beam elements, *Comput. Methods Appl. Mech. Engrg.* 81 (1990) 131–150.
- [22] K.S. Schweizerhof and E. Ramm, Displacement dependent pressure loads in nonlinear finite element analysis, *Comput. Struct.* 18 (1984) 1099–1114.
- [23] K.J. Bathe, *Finite Element Procedure in Engineering Analysis* (Prentice-Hall, Englewood Cliffs, NJ, 1982).
- [24] K.M. Hsiao, Nonlinear buckling analysis of 3-D beams by the FEM, *Summaries of Papers, Conference on the Mathematics of Finite Elements and Applications held at Brunel Institute of Computational Mathematics, Brunel, 25–28 June 1995.*
- [25] Y. Goto, X.S. Li and T. Kasugal, Buckling analysis of elastic space rods under torsional moment, *J. Engrg. Mesh. ASCE* 122 (1996) 826–833.